Pseudorandom Code-Aided Acquisition and Tracking of Globalstar Satellite Signals for Opportunistic Navigation

Xing Liu*, José A. López-Salcedo†, Gonzalo Seco-Granados†, Tareq Y. Al-Naffouri*
*King Abdullah University of Science and Technology (KAUST), Thuwal, Saudi Arabia
†Universitat Autònoma de Barcelona (UAB), IEEC-CERES, Barcelona, Spain

***Abstract*—Opportunistic navigation using low Earth orbit (LEO) satellites has emerged as a promising alternative and complement to global navigation satellite systems (GNSS). Globalstar is a noteworthy LEO constellation for this application, as it employs a spread-spectrum modulation principle similar to that used in most GNSS systems. A significant challenge in processing Globalstar signals lies in the absence of documented specifications on the spreading code sequences. This paper explores an approach to deriving these codes using the limited available information. It then examines the acquisition and tracking of Globalstar satellite signals for opportunistic navigation. The experimental results validate the successful generation of the pseudorandom codes and the reliability of the signal acquisition and tracking process, highlighting the potential of Globalstar satellites for navigation applications.**

***Index Terms*—Globalstar, LEO satellite, opportunistic navigation, spreading codes.**

I. Introduction

In recent years, low Earth orbit (LEO) satellites have drawn considerable attention due to their potential to augment global navigation satellite system (GNSS) systems or serve as a reliable backup in the event of GNSS failures [1]. Their closer proximity to Earth enhances received signal power, which not only improves positioning accuracy but also provides robust resistance against disruptions like jamming and spoofing. Companies such as SpaceX, OneWeb, Globalstar, and others, along with government organizations, are actively deploying and expanding their LEO satellite constellations, with thousands of satellites already available. The vast number of LEO satellites, coupled with the diversity of their signals, offers significant benefits for improving positioning reliability and accuracy.

New LEO constellations specifically designed for positioning, navigation, and timing (PNT) services are still in the early stages of development. Different signal structures are being explored for LEO-PNT applications, including GNSS-like, orthogonal frequency-division multiplexing (OFDM), and chirp spread spectrum (CSS) signals [2]. In contrast, utilizing existing LEO constellations for navigation in an opportunistic manner offers a promising alternative [3]. These constellations, despite being originally designed for broadband internet, teleservices, IoT applications, and more, can be utilized for positioning without requiring changes to the existing satellite infrastructure. However, specialized signal processing and receiver architecture are necessary to enable this functionality. Among these existing constellations, Globalstar is particularly interesting due to its use of the spread-spectrum modulation principle, similar to most GNSS systems [4], [5]. As such, the receiver architecture for Globalstar signals shares many similarities with that of GNSS receivers, enabling the adaptation of existing GNSS signal processing techniques and thereby bridging the gap between conventional GNSS-based and LEO-based positioning. Furthermore, investigating Globalstar for opportunistic navigation can offer insights into the design of LEO PNT constellations with GNSS-like signals, as well as offer guidance for developing integrated positioning and communication systems via LEO satellites.

Despite the similarities between Globalstar and GNSS signal structures, a significant challenge lies in the lack of publicly available signal specifications. The spreading sequence structure of a specific Globalstar code division multiple access (CDMA) channel consists of an inner pseudorandom noise (PN) sequence pair and a single outer PN sequence [4], [6]. These PN sequences serve as unique identifiers that allow the receiver to distinguish individual satellites, synchronize with their signals, and facilitate precise observations for navigation. However, the specific PN sequences employed by Globalstar remain undisclosed, hindering their use for navigation applications.

Several strategies have been developed to address the challenge of undisclosed PN sequences by Globalstar. The technique presented in [7] eliminates the spreading code by raising the received signal to the fourth power, thereby neutralizing the QPSK modulation in both the in-phase and quadrature components of Globalstar signals. The study in [8] examines Doppler stretch estimation and compensation for Globalstar, but does not present the PN sequence. Additionally, a blind spectral approach has been proposed for opportunistic positioning using unknown LEO satellite signals [9]. In contrast to existing works, this paper provides new insights and more details on the generation of Globalstar spreading codes,

This work has been partly supported by the King Abdullah University of Science and Technology (KAUST) Office of Sponsored Research (OSR) under Award ORA-CRG2021-4695, and in part by the Spanish Agency of Research (AEI) under grant PID2023-152820OB-I00 funded by MICIU/AEI/10.13039/501100011033 and by ERDF/EU, and grant PDC2023-145858-I00 funded by MICIU/AEI/10.13039/501100011033 and by the European Union NextGenerationEU/PRTR.

serving as a follow-up to [10].

In this paper, we first present the signal model of Globalstar satellites. We make use of the PN sequences derived from the limited public information available about Globalstar signal specifications. Using the derived PN sequences, we generate local replica sequences and perform correlation with satellite signals to carry out the acquisition process. Subsequently, fine alignment is applied to precisely track variations in code delay, carrier phase, and Doppler shift caused by satellite movement and user dynamics. The proposed method is evaluated using recorded samples from live Globalstar satellite signals, with its effectiveness validated by acquisition and tracking results.

II. Globalstar Signal Model

Globalstar satellites utilize CDMA technology for satellite phone services and low-speed data communications. Operating within the S-band range of 2483.5 to 2500 MHz, Globalstar satellite-to-user links encompass a total bandwidth of 16.5 MHz [4]. The same frequency set is consistently used across 16 beams. Each beam is subdivided into 13 frequency division multiplexing (FDM) slots, known as subbeams, each with a bandwidth of 1.23 MHz.

Each Globalstar CDMA channel incorporates a pair of inner PN sequences and a single outer PN sequence [4]. The inner PN sequences are employed to identify the orbital plane, with one sequence allocated for spreading the in-phase signal component and the other for the quadrature component. Each inner PN sequence has a length of 1024 chips and operate at a chip rate of 1.2288 Mcps. In contrast, the outer PN sequence features a length of 288 chips and a chip rate of 1.2 kcps. Each outer PN chip encompasses exactly one complete period of the inner PN sequence. The outer PN sequence modulates the inner PN sequence to generate the final spreading sequence, which spans a duration of 240 milliseconds. Additionally, coherent transmissions are implemented using CDMA Walsh codes, which comprise 128 orthogonal code channels. The forward CDMA channel is structured to include the pilot channel, paging channels, sync channels, and traffic channels. Specifically, the pilot channel employs an all-zeros Walsh code. This spreading and modulation mechanism is applied consistently across all forward link channels. The in-phase and quadrature baseband signals are subsequently modulated onto a carrier signal for transmission within each subbeam. In this paper, we focus on the pilot channel for opportunistic navigation.

Based on the signal structure outlined earlier, the equivalent Globalstar pilot signal can be expressed as

$$s(t) = \left(x_{\mathrm{I}}(t) + j x_{\mathrm{Q}}(t)\right) e^{j2\pi f_{\mathrm{c}} t}, \tag{1}$$

Here, j is the imaginary unit, and f_{c} denotes the carrier frequency. $x_{\mathrm{I}}(t)$ and $x_{\mathrm{Q}}(t)$ are the in-phase and quadrature components, respectively, which can be further defined using the inner and outer spreading codes as follows:

$$x_{\mathrm{I}}(t) = \sum_{m=0}^{N_v-1} \sum_{k=0}^{N_c-1} v[m] c_{\mathrm{I}}[k] p\left(t - kT_c - mT_v\right), \tag{2}$$

$$x_{\mathrm{Q}}(t) = \sum_{m=0}^{N_v-1} \sum_{k=0}^{N_c-1} v[m] c_{\mathrm{Q}}[k] p\left(t - kT_c - mT_v\right), \tag{3}$$

where $\{c_{\mathrm{I}}[k]\}_{k=0}^{N_{\mathrm{c}}-1}$ and $\{c_{\mathrm{Q}}[k]\}_{k=0}^{N_{\mathrm{c}}-1}$ are the inner PN sequences with a length of $N_{\mathrm{c}} = 1024$ chips and a chip period T_{c}, $\{v[k]\}_{m=0}^{N_{\mathrm{v}}-1}$ is the outer PN sequence with $N_v = 288$ chips and a chip period $T_v = N_c T_c$, and $p(t)$ characterizes the chip pulse waveform.

The received Globalstar pilot signal can be modeled as

$$r(t) = \alpha s\left(\left(1 + f_{\mathrm{d}}/f_{\mathrm{c}}\right) t - \tau_t\right) + w(t), \tag{4}$$

where α represents the channel gain, f_{d} is the Doppler frequency shift, and $w(t)$ is the additive noise. The presence of Doppler shift leads to compression or expansion of the time-domain signal. Although this effect is typically negligible for GNSS, it requires careful consideration for LEO satellites because of their high dynamics.

After signal conditioning, the discrete-time baseband model of the received Globalstar pilot signal can be represented as

$$\begin{aligned} r[n] = \alpha\big(&x_{\mathrm{I}}[(1+f_{\mathrm{d}}/f_{\mathrm{c}})n - \tau] + j x_{\mathrm{Q}}[(1+f_{\mathrm{d}}/f_{\mathrm{c}})n - \tau]\big) \\ &\cdot e^{j(2\pi \frac{f_{\mathrm{d}}}{F_{\mathrm{s}}} n + \theta)} + w[n], \end{aligned} \tag{5}$$

where $r[n] = r\left(nT_{\mathrm{s}}\right)$ denotes the discrete-time version of the received signal, F_{s} is the sampling frequency, $T_{\mathrm{s}} = 1/F_{\mathrm{s}}$ is the sampling time, τ represents the discrete-time counterpart of the continuous-time delay, and θ is the carrier phase.

To compute range measurements for positioning and navigation, the receiver must first achieve frequency and time synchronization with the satellite signals. A key challenge of processing Globalstar signals arises from the lack of publicly available information on the inner and outer spreading codes.

III. Spreading Code Generation, Signal Acquisition, and Tracking

In this section, we first explore a potential way to derive Globalstar spreading codes by leveraging the limited available information and the signal model outlined in Section II, which enables the subsequent processes of signal acquisition and tracking.

A. Generation of Globalstar Spreading Codes

Globalstar inner PN sequences are composed of 1024 chips, yet specific details on their generation remain undisclosed. Considering their length, one feasible method could involve employing 10-bit polynomials for linear feedback shift registers (LFSRs) to produce a PN sequence of 1023 chips, with an additional chip added to reach the full length. Table I presents a list of 10-bit polynomials in hexadecimal format, used in LFSRs for generating maximal-length PN sequences.

Using the polynomials in Table I, LFSRs can generate PN sequences with a period of 1023 chips, to which an additional chip is inserted at various positions within the sequence. This approach enables the generation of spreading codes that match the length employed by Globalstar satellites. Moreover, the sequence can be either direct or reversed, the inserted chip can be 0 or 1, and different sequence offsets may be applied

TABLE I
LIST OF 10-BIT POLYNOMIALS FOR LFSRS GENERATING MAXIMAL-LENGTH PN SEQUENCES

204	20D	213	216	232	237	240	245	262	26B
273	279	27F	286	28C	291	298	29E	2A1	2AB
2B5	2C2	2C7	2CB	2D0	2E3	2F2	2FB	2FD	309
30A	312	31B	321	327	32D	33C	33F	344	35A
360	369	36F	37E	38B	38E	390	39C	3A3	3A6
3AA	3AC	3B1	3BE	3C6	3C9	3D8	3ED	3F9	3FC

as well. Considering all these possibilities, we can construct the potential PN sequences.

B. Correlation Analysis and Signal Acquisition

To assess the effectiveness of these PN sequences, we use them along with tentative values for time delay and Doppler frequency shift, denoted as $\{\tau', f'_{\mathrm{d}}\}$, to generate local replicas of the satellite signal and compute their correlation with the received signal. The replica consists of both code and carrier components. At this stage, we initially disregard the outer code to focus solely on the inner spreading code. Rather than evaluating a pair of PN sequences jointly, we assess each one individually. Additionally, for simplicity, signal compression and expansion are initially ignored but will be considered during the tracking process for more precise estimations. Consequently, we proceed to the following circular correlation analysis

$$R_{\mathrm{C}}\left(\tau', f'_{\mathrm{d}}\right) = \frac{1}{N_T} \sum_{n=0}^{N_T-1} r[n] c^{*}\left[n-\tau'\right]_{N_{\mathrm{c}}} e^{-j2\pi \frac{f'_{\mathrm{d}}}{F_{\mathrm{s}}} n}, \quad (6)$$

where $c[n] = c\left(nT_{\mathrm{s}}\right)$ denotes the discrete-time spreading code, $e^{-j2\pi \frac{f'_{\mathrm{d}}}{F_{\mathrm{s}}} n}$ corresponds to the discrete-time complex carrier due to the Doppler frequency shift f'_{d}, and N_T represents the coherent integration length. The subscript N_{c} indicates that the indexing of the code replica is cyclic or modular, with a period of N_{c}, keeping indices within the bounds $0 \leq |n-\tau'| \leq N_{\mathrm{c}}-1$. As a result, τ' represents only the fractional part of the actual time delay within one code cycle.

Given that both the received signal $r[n]$ and the local carrier replica are complex, the correlation outcome $R_{\mathrm{C}}\left(\tau', f'_{\mathrm{d}}\right)$ is complex as well. If the estimated values $\{\tau', f'_{\mathrm{d}}\}$ closely approximate the true ones, the received signal aligns well with the local replica generated with the correct PN sequence, leading to a high correlation magnitude $|R_{\mathrm{C}}\left(\tau', f'_{\mathrm{d}}\right)|$. The process of evaluating potential PN sequences is similar to GNSS signal detection but involves greater complexity due to the unknown PN sequences and the larger Doppler shifts caused by the high dynamics of Globalstar satellites operating in LEO. Given the high computational complexity, we employ a full parallel search algorithm leveraging fast fourier transform (FFT) operations to improve efficiency [11]. The procedure is outlined as follows:

1) Generate a candidate spreading code $c[n]$ using LFSRs based on the polynomials listed in Table I, with the option to keep it direct or reverse it, inserting an additional chip (1 or 0) at various positions within the sequence.
2) Apply the FFT to $c[n]$ and take the complex conjugate. The complex conjugate operation is required to perform the correlation operation in the frequency domain.
3) Multiply the received signal $r[n]$ by a locally generated carrier wave $e^{-j2\pi \frac{f'_{\mathrm{d}}}{F_{\mathrm{s}}} n}$ to mitigate the frequency shift present in $r[n]$. Subsequently, compute the FFT of the resulting signal.
4) Compute $R_{\mathrm{C}}(\tau', f'_{\mathrm{d}})$ by multiplying the output from Step 2 with that of Step 3, and then applying an inverse FFT (IFFT).
5) For a specific $c[n]$, repeat Steps 3 and 4 to calculate $R_{\mathrm{NC}}(\tau', f'_{\mathrm{d}})$ across various tentative frequency values f'_{d}.
6) Repeat steps 1 through 4 to compute $R_{\mathrm{NC}}(\tau', f'_{\mathrm{d}})$ for all candidate spreading codes.

Through correlation analysis, we can identify the generation mechanism of Globalstar's inner PN sequences. Once the correct PN sequences are recognized, we can detect the presence of target satellite signals and roughly estimate their Doppler shifts and code delays through similar correlation analysis. This process is known as acquisition.

C. Signal Tracking

Once the acquisition process is completed, the coarse estimates of code delay and frequency shift are utilized as inputs to the tracking stage, which then refines these estimates and continuously monitors potential variations over time. The tracking stage consists of two modules: one for carrier tracking and the other for code tracking. In this work, a frequency-locked loop (FLL) is initially used for carrier tracking, transitioning to a phase-locked loop (PLL) once steady-state is reached for finer tracking. A delay-locked loop (DLL) is employed for code tracking. Due to the high dynamics of the Globalstar satellites, which cause significant Doppler shifts in the signals, a third-order PLL, along with a second-order FLL and a second-order DLL, is used to accurately track the carrier phase and frequency variations.

IV. EXPERIMENTAL RESULTS

This section presents the experimental results obtained from a dataset of live recordings from Globalstar satellites gathered on November 8, 2022. The dataset was obtained by pointing a big dish antenna to individual Globalstar satellites, and recording the subbeam 9 centered at 2494.23 MHz with a sampling frequency of 12.5 MHz.

A. Validation of Spreading Code Generation

Before processing the live Globalstar signals, we first present a simulation result to serve as a reference for validating the feasibility of the approach in generating inner spreading codes. Fig. 1 shows the correlation between two sequences. The first sequence is generated using a 10-bit polynomial for

TABLE II
POLYNOMIAL PAIRS CORRESPONDING TO EFFECTIVE PN SEQUENCE GENERATION FOR GLOBALSTAR SATELLITES

Polynomial Pairs	32D & 3A3	232 & 390	213 & 298
Satellite ID	M073	M074	M078
	M076	M075	M084
	M081	M077	M085
	M083	M079	M086
	M088	M080	M089
	M090	M082	M092
	M093	M091	M094
		M095	
		M096	
		M097	

an LFSR that produces a PN sequence with 1023 chips, with an additional zero chip appended to the end of the sequence. The second sequence is similarly generated using the same 10-bit polynomial for an LFSR, producing a PN sequence with 1023 chips, but with the zero chip inserted at various positions within the sequence. The maximum correlation occurs when the second sequence with the additional chip aligns with the position of the zero chip in the first sequence. A 'V' shape is observed as the position of the additional chip in the second sequence varies.

Now, we proceed with the analysis of the live Globalstar signals. Based on the correlation analysis, we identified pairs of inner PN sequences that result in sufficiently high correlation outcomes for the Globalstar satellites present in the dataset. These PN sequences are generated using LFSRs with specific polynomials and an initial state $\begin{bmatrix}0 & 0 & 0 & 0 & 0 & 0 & 0 & 0 & 0 & 1\end{bmatrix}$, then reversed, and an additional zero chip is appended to the end of each sequence. The polynomial pairs working for various satellites are summarized in Table II. Specifically, Fig. 2 presents the correlation results between signals from Globalstar satellite M073 and PN sequences generated by LFSRs with polynomials 32D and 3A3, with an additional chip inserted at various positions within the generated sequence. Here, we implement coherent correlation over one period of the inner PN sequence, without considering non-coherent accumulation. This figure highlights the high correlation values between the real signal and the local replica. Moreover, the consistent trends between Fig.1 and Fig.2 validate that our generated sequences match those used by Globalstar.

B. Identification of Code Offsets

When the additional chip is appended to the start or end of a sequence, the correlation values in Fig.2 remain identical due to the properties of circular correlation. Additionally, a PN code offset may be used to distinguish satellites and signal beams [12]. To investigate this further, we conduct a correlation analysis using PN sequences with the additional chip appended to the end, applying different offsets. A time window is then slid to align the real signal sequences with the PN sequence, that is, the code phase associated with the correlation peak is set to zero. In this configuration, the correct offset yields the highest correlation value, as it

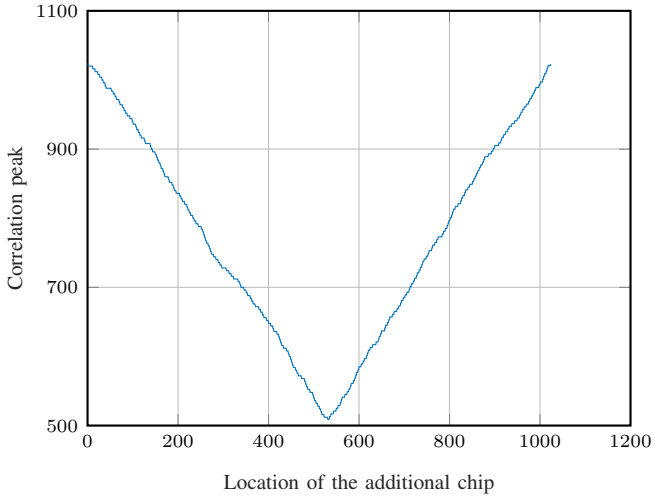

Fig. 1. Correlation analysis of two locally generated PN sequences using the same 10-bit polynomial LFSR: one with a zero chip added to the end, and the other with the zero chip inserted at various positions.

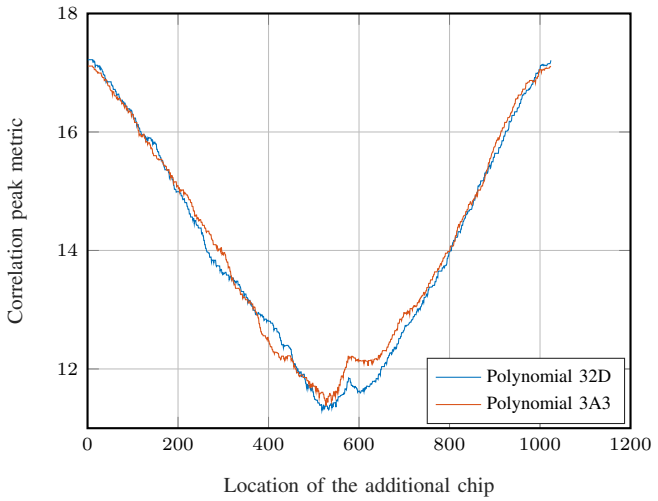

Fig. 2. Correlation between live Globalstar M073 signal and PN sequences locally generated with LFSRs using polynomials 32D and 3A3 with an additional chip inserted at various locations.

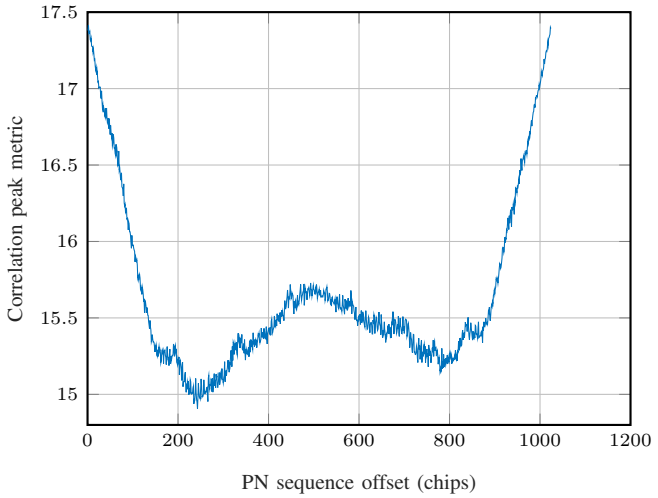

Fig. 3. Correlation analysis as a function of different PN sequence offsets.

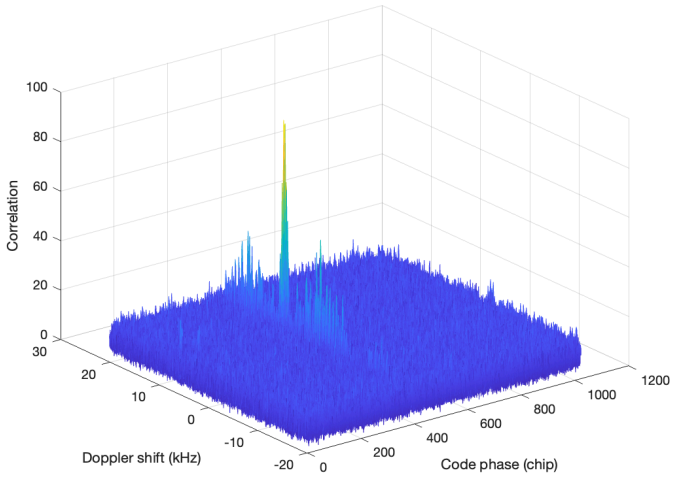

Fig. 4. Correlation function for signal acquisition.

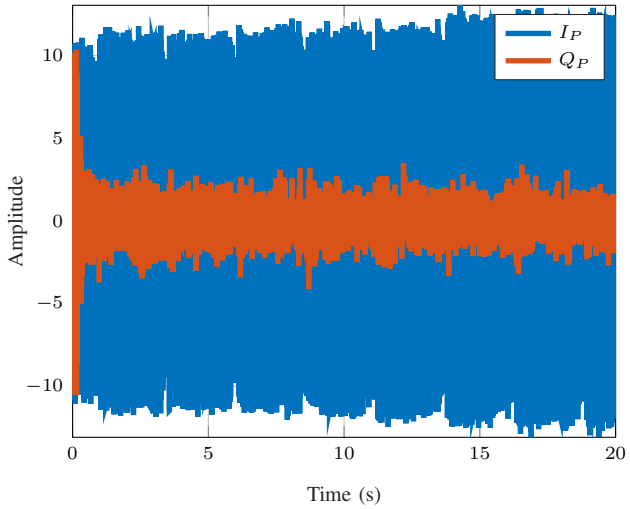

Fig. 6. In-phase (I_P) and quadrature (Q_P) prompt correlator outputs.

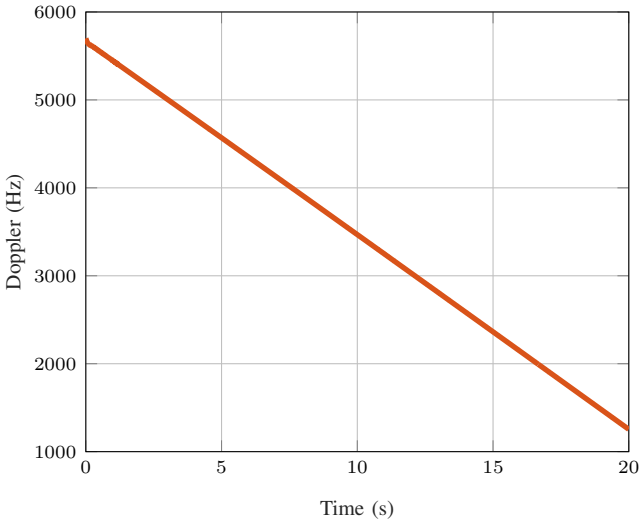

Fig. 5. Estimated Doppler frequency.

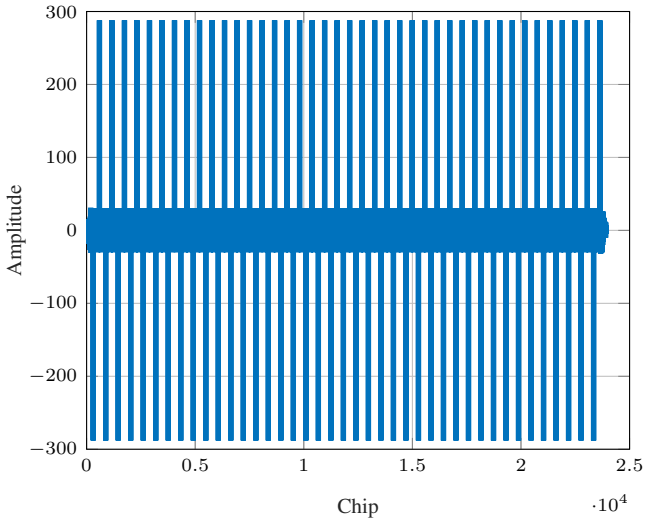

Fig. 7. Correlation between the estimated outer PN sequence and its last 288 chips.

eliminates the impact of the sign change in the outer PN sequence. Fig.3 presents the correlation values for Globalstar M073 as a function of PN sequence offsets, generated using polynomial 32D. The highest correlation is achieved at zero offset, indicating that the additional chip is appended to the end and no offset is applied for the considered satellite subbeam.

C. Signal Acquisition and Tracking Results

Having recognized the PN sequences, we proceed with signal acquisition and tracking. The Finnish Geospatial Research Institute GNSS Software Receiver (FGI-GSRx) [11] is modified to process Globalstar signals. Fig. 4 presents the correlation results across the two-dimensional search space corresponding to the determined PN sequence. The correlation is computed using 6 periods of the inner PN sequence for coherent correlation and 4 non-coherent accumulations. The sharp correlation peak confirms successful signal acquisition, precisely identifying both the Doppler shift and code phase needed for signal synchronization. Subsequently, the tracking process is performed to continuously refine the Doppler shift and code phase estimates over time. Fig.5 illustrates the estimated Doppler frequency shift during tracking stage, showing its rapid variations. Since only a single PN sequence is utilized instead of a pair, only the in-phase signal component is tracked, as verified by the in-phase and quadrature prompt correlator outputs shown in Fig. 6. These results from the prompt correlators demonstrate the success of signal tracking.

Once the signal is tracked and synchronized, the outer code symbols can be detected. The estimated sequence exhibits periodic repetition, with its period matching the documented period of the Globalstar outer PN sequence. To highlight this periodicity, Fig. 7 illustrates the correlation between the estimated outer PN sequence and its last 288 chips. This figure shows distinct periodic peaks every 288 chips. Additionally, it indicates that the overall sign of the 288-chip outer PN sequence alternates between +1 and -1 with each period.

V. Conclusions

This paper explores the potential of using Globalstar LEO satellites for opportunistic navigation. In addition to the inherent advantages of LEO satellites over higher-orbit satellites, the similarity between Globalstar's signal structure and that of traditional GNSS systems makes its signals a promising candidate for integration into navigation solutions. The potential mechanism for deriving the publicly unknown spreading codes used in Globalstar signals is presented. The experimental results validate the effectiveness of the generated pseudorandom sequences, enabling reliable signal acquisition and tracking of Globalstar satellites. These findings underscore the feasibility of incorporating Globalstar satellites into navigation systems.

Acknowledgment

The authors wish to express their gratitude to the Navigation Laboratory at the European Space Research and Technology Centre (ESTEC) in Noordwijk, The Netherlands, for providing recorded samples of Globalstar signals.

References

[1] Y. J. Morton, F. van Diggelen, J. J. Spilker Jr, B. W. Parkinson, S. Lo, and G. Gao, *Position, navigation, and timing technologies in the 21st century: Integrated satellite navigation, sensor systems, and civil applications, volume 1*. John Wiley & Sons, 2021.

[2] D. Egea-Roca, J. A. López-Salcedo, and G. Seco-Granados, "Performance analysis of the pilot and data component of a CSS signal for LEO-PNT," *Engineering Proceedings*, vol. 54, no. 1, p. 35, 2023.

[3] W. Stock, R. T. Schwarz, C. A. Hofmann, and A. Knopp, "Survey on opportunistic PNT with signals from LEO communication satellites," *IEEE Communications Surveys & Tutorials*, pp. 1–1, 2024.

[4] L. Schiff and A. Chockalingam, "Signal design and system operation of Globalstar™ versus IS-95 CDMA–similarities and differences," *Wireless Networks*, vol. 6, pp. 47–57, 2000.

[5] P. Teunissen and O. Montenbruck, *Springer handbook of global navigation satellite systems*. Springer, 2017.

[6] R. De Gaudenzi, "Payload nonlinearity impact on the Globalstar forward link multiplex. i. physical layer analysis," *IEEE Transactions on Vehicular Technology*, vol. 48, no. 3, pp. 960–976, 1999.

[7] Y. Zhang, H. Qin, and G. Shi, "Doppler positioning based on Globalstar signals of opportunity," in *2023 5th International Conference on Electronic Engineering and Informatics (EEI)*, 2023, pp. 666–669.

[8] M. Neinavaie, J. Khalife, and Z. M. Kassas, "Doppler stretch estimation with application to tracking Globalstar satellite signals," in *MILCOM 2021 - 2021 IEEE Military Communications Conference (MILCOM)*, 2021, pp. 647–651.

[9] S. Kozhaya, H. Kanj, and Z. M. Kassas, "Multi-constellation blind beacon estimation, Doppler tracking, and opportunistic positioning with OneWeb, Starlink, Iridium NEXT, and Orbcomm LEO satellites," in *2023 IEEE/ION Position, Location and Navigation Symposium (PLANS)*, 2023, pp. 1184–1195.

[10] O. Peña, G. Seco-Granados, and J. A. López-Salcedo, "Coherent tracking of Globalstar signals using partially-known spreading codes," in *2024 ESA Workshop on Satellite Navigation User Equipment Technologies (NAVITEC)*, 2024, pp. 1–5.

[11] K. Borre, I. Fernández-Hernández, J. A. López-Salcedo, and M. Z. H. Bhuiyan, *GNSS software receivers*. Cambridge University Press, 2022.

[12] P. A. Monte, R. A. Wiedeman, and M. J. Sites, "Method for accounting for user terminal connection to a satellite communications system," Sep. 2 1997, US Patent 5,664,006.